CSIRO PUBLISHING

Australian Journal of Physics

Volume 53, 2000

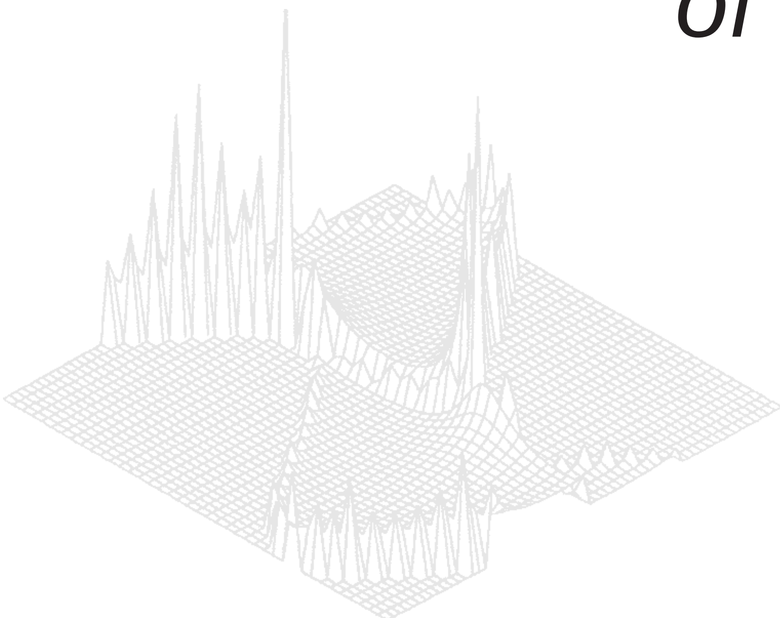

A journal for the publication of
original research in all branches of physics

www.publish.csiro.au/journals/ajp

All enquiries and manuscripts should be directed to
Australian Journal of Physics
CSIRO PUBLISHING
PO Box 1139 (150 Oxford St)
Collingwood
Vic. 3066
Australia

Telephone: 61 3 9662 7626
Facsimile: 61 3 9662 7611
Email: peter.robertson@publish.csiro.au

CSIRO AUSTRALIA

Published by **CSIRO** PUBLISHING
for CSIRO and
the Australian Academy of Science

Academy of Science

Aust. J. Phys., 2000, **53**, 463–476

Absorptive Quantum Measurements via Coherently Coupled Quantum Dots*

G. J. Milburn, H. B. Sun and B. Upcroft

Department of Physics, University of Queensland,
St Lucia, Qld 4067, Australia.

Abstract

We propose an absorptive measurement scheme via coupled quantum dots based on studies of the quantum dynamics of coherently coupled dots. The system is described through a Markov master equation that is related to a measurable quantity, the current. We analyse the measurement configuration and calculate the correlations and noise spectra beyond the adiabatic approximation.

1. Introduction

In traditional condensed matter physics, quantum measurement issues rarely arise as one is typically making measurements on ensembles of systems for which spatial and other inhomogeneities dominate. Recent experiments in mesoscopic electronics have begun to probe fundamental issues in quantum measurement (Buks *et al*. 1998; Sprinzak *et al*. 1999) and there is a large and growing literature on theoretical models of such experiments (Wiseman *et al*. 2000; Elattari and Gurvitz 2000). However, recently it has become possible to make repeated measurements on a single quantum system. In such a context the measurement induced fluctuations can dominate the dynamics of the device and one must take into account the conditional dynamics in which the state at any time is conditioned by the results of the previous measurement. This is especially true of a class of measurements called *welcher weg* or 'which path' experiments where an attempt is made to determine which of two or more paths a particle has taken inside a quantum interferometor (Buks *et al*. 1998; Aleiner *et al*. 1997). Experiments of this kind have become possible due to the special features of mesoscopic electronic devices. Such devices are comparable or smaller than certain characteristic lengths, namely (1) the de Broglie wavelength, (2) the mean free path, and (3) the phase-relaxation length (Datta 1995). The classical laws describing electronic components break down and quantum effects begin to dominate. Devices of this size exist in a domain where the classical and quantum realms meet and so are termed mesoscopic. In this paper we are primarily concerned with quantum transport in coupled quantum dots.

Coupled quantum dots have a wide range of applications and potential. Some of these applications include generation of terahertz radiation (Luryi 1991), electron pumping (Blick *et al*. 1996), temperature modulator in the phonon environment (Fujisawa and Tarucha 1997), and devices for studying dephasing mechanisms in high precision measurements (Gurvitz 1997). In certain configurations, quantum dots can be used to employ

* Refereed paper based on a contribution to the Ninth Gordon Godfrey Workshop on Condensed Matter in Zero, One and Two Dimensions held at the University of New South Wales, Sydney, in November 1999.

 10.1071/PH00034 0004-9506/00/040463$05.00

classical Boolean logic, i.e. create classical logic gates (Lent and Tougaw 1993; Bandyopadhyay *et al.* 1994; Openev and Bychkov 1998). For example, an AND/OR logic gate can be composed of a pair of tunnel-coupled quantum dots where the vacancy and occupation of the dot by a single electron represented a bit 0 and 1 respectively (Nomoto *et al.* 1996). Quantum dots may also be the basis for quantum computation schemes. Implementation of a quantum gate in solid state devices involves a quantum bit (qubit) to exist in any state of a quantum two-level system such that it is entangled with another qubit. Entanglement can be achieved between electrons in two separate quantum dots if the dots are coupled coherently.

In mesoscopic electron transport, shot noise is dominant (Milburn and Sun 1998). The Pauli exclusion principle and Coulomb blockade can induce strong correlations between carriers resulting in current noise suppression. In studying the characteristics of correlations in quantum dots we use a quantum stochastic treatment to show how the observed classical stochastic process is conditioned on the quantum stochastic process involving tunnelling of electrons.

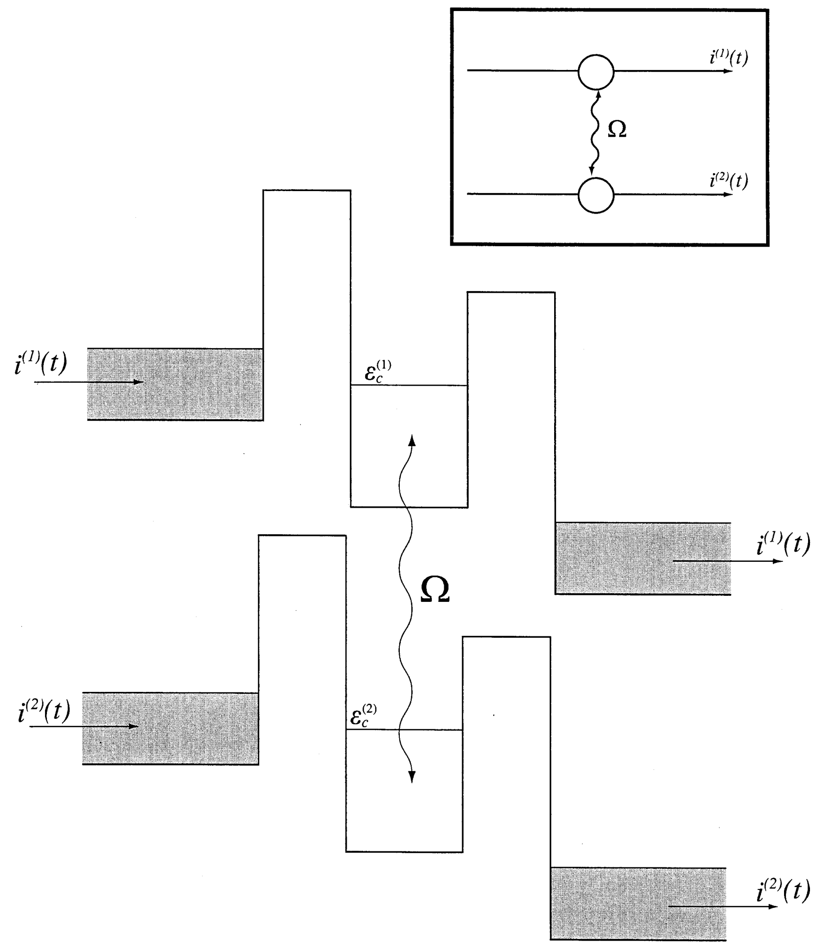

Fig. 1. Two single quantum dots coherently coupled in parallel. The inset is a schematic representation of the coupled dots.

In this paper we consider a possible quantum measurement system that could be realised using two coherently coupled quantum dots. Each dot is also coupled to a separate external lead giving a four terminal configuration. The source/drain system for each quantum dot is modelled as a fermionic heat bath.

We use a similar quantum stochastic description to that which we used previously (Sun and Milburn 1999) in describing noise in double quantum dots and measurements of quantum coherence using a single electron transistor.

The system we consider is shown schematically in Fig. 1. A potential barrier separates two dots through which the electrons can tunnel coherently. Each dot is coupled to its own source and drain, which represent Fermi heat baths in local thermodynamic equilibrium. An overall bias potential maintains a differential chemical potential between the source and the drain. We regard dot-1 as the measurement apparatus and dot-2 as the measured system (we could equally have taken these the other way around). The Hamiltonian describing the coupled dots is given by

$$
\begin{aligned}
H = & \sum_k \varepsilon_k^{(s)} a_k^\dagger a_k + \sum_l \varepsilon_p^{(d)} b_l^\dagger b_l + \sum_k \varepsilon_k^{(s)} s_k^\dagger s_k + \sum_l \varepsilon_p^{(d)} t_l^\dagger t_l \\
& + \varepsilon_1 c_1^\dagger c_1 + \varepsilon_2 c_2^\dagger c_2 \\
& + \sum_k \left(A_k c_1^\dagger a_k + A_k^* a_k^\dagger c_1 \right) + \sum_k \left(B_k c_1^\dagger b_k + B_k^* b_k^\dagger c_1 \right) \\
& + \sum_p \left(S_l s_l^\dagger c_2 + S_l^* c_2^\dagger s_l \right) + \left(T_l t_l^\dagger c_2 + T_l^* c_2^\dagger t_l \right) \\
& + \hbar\Omega \left(c_1^\dagger c_2 + c_2^\dagger c_1 \right) ,
\end{aligned}
\tag{1}
$$

where a_k, b_k are Fermi field operators (i.e they obey the usual anti-commutation relations) for the source and drain reservoirs of dot-1 respectively, and similarly s_k, t_k are Fermi field operators for the source and drain reservoirs of dot-2. The free energies of each dot are ε_1, ε_2 respectively, and $n = 1, 2$ labels each dot. The coupling constants A_k, B_k, S_k, T_k depend on the detailed band structure that forms the barriers and the bias conditions. We will assume that the coupling is sufficiently weak that the resulting broadening of the bound states of each dot is small compared to the energy gap between the bound state and the top of the Fermi surface in the source and the drain for each dot.

We now assume that each reservoir (source and drain) for each dot is in local thermodynamic equilibrium and that further the bound states of each dot are below the Fermi surface in the source and above the Fermi surface in the drain. This is an effective 'zero temperature' limit. The density operator of the whole system in the interaction picture then obeys the equation of motion $dR/dt = -(i/\hbar)[H, R]$ and can be solved using the same technique as in Sun and Milburn (1999). As a result the quantum master equation for the coupled quantum dots is

$$
\frac{dR}{dt} = -i\Omega[c_1^\dagger c_2 + c_1 c_2^\dagger, R] + \sum_{n=1}^{2} (\gamma_{Ln} \mathcal{D}[c_n^\dagger] R \tag{2}
$$

$$
+ \gamma_{Rn} \mathcal{D}[c_n] R), \tag{3}
$$

where we have defined the superoperator $\mathcal{D}[A]R = ARA^\dagger - (A^\dagger AR + RA^\dagger A)/2$ and γ_{Ln}, γ_{Rn} are the incoherent tunnelling rates from the Fermi reservoirs into and out of each dot.

In an experiment the measured quantities are classical currents and voltages in the leads of the device containing the dot. We need to relate these classical stochastic processes to the quantum dynamics on the dot as given by the master equation. This connection is given by Milburn (2000). The emission of an electron from the source lead into the dot causes an electron to be drawn into this reservoir to maintain local thermodynamic equilibrium. This results in a current spike in the source. This is an entirely classical stochastic process which in the limit of a very fast response in the source circuit may be approximated by a point process $dN_s(t)$ (Gardiner 1983). The random variable $edN_s(t)$ is the increment in the charge in the source between t and $t + dt$. It was shown by Milburn (2000, see present issue p. 477) that this point process is conditioned by *anti-normal* ordered Fermi field operators in the source reservoir. When an electron is emitted from the dot in the drain, it must be instantaneously removed (absorbed) by the external circuit to maintain local thermodynamic equilibrium in the drain. As for the source, in the limit of fast response of the drain circuit we can approximate this by a classical point process $dN_D(t)$, where $edN_D(t)$ is the change in charge in the drain between t and $t + dt$. This point process is conditioned on *normally* ordered Fermi field operators in the drain reservoir. The Ramo–Shockley theorem (Ramo 1939; Shockley 1938) can be used to find the current increment that flows in the external circuit when a charge increment occurs in the source and drain lead due to tunnelling into and out of the dot. In the case of a symmetric device the instantaneous current in the external circuit containing dot-n is related to the charge increments by

$$i_n(t)dt = \frac{e}{2}\left(dN_{Sn}(t) + dN_{Dn}(t)\right). \tag{4}$$

It then follows (Milburn 2000) that the average current in the external circuit containing dot-n is determined by quantum averages on the dot itself,

$$E(i_n(t)) = \frac{e}{2}\left(\gamma_{Ln}\langle c_n c_n^\dagger\rangle + \gamma_{Rn}\langle c_n^\dagger c_n\rangle\right). \tag{5}$$

2. Measurement Configuration

We will first describe a simpler configuration to illustrate how this system can function as a quantum limited measurement. In the measurement configuration we assume that dot-1 is the measurement *apparatus*, while dot-2 is the system to be measured. The objective of the measurement is to determine the occupation of dot-2. To this end assume that the bias on the second dot is changed so that it is no longer coupled to external currents. We will further assume that electrons leave the apparatus dot (dot-1) much faster than the tunnelling rate between the two dots. In this case we adiabatically eliminate the dynamics of the apparatus dot by assuming that it remains close to a steady state at all times. This enables us to give a single master equation for the measured dot which has the characteristic form of an open measured system.

The master equation for the combined density operator of the system and apparatus, R, is

$$\frac{dR}{dt} = -i\Omega[c_1^\dagger c_2 + c_1 c_2^\dagger, R] + \gamma_{L1}\mathcal{D}[c_1^\dagger]R + \gamma_{R1}\mathcal{D}[c_1]R. \tag{6}$$

We now assume that $\gamma_{L1}, \gamma_{R1} >> \Omega$ and make the ansatz for $R(t)$

$$
\begin{aligned}
R(t) \approx\ & \rho_{00}(t) \otimes |0\rangle_1\langle 0| + \rho_{11}(t) \otimes |1\rangle_1\langle 1| \\
& + \rho_{10}(t) \otimes |1\rangle_1\langle 0| + \rho_{01}(t) \otimes |0\rangle_1\langle 1|,
\end{aligned}
\tag{7}
$$

where $|n\rangle_1$ is a particle number eigenstate for dot-1. Note that ρ_{nm} is an operator acting in the Hilbert space of the measured system (dot-2). The reduced system density operator describing the measured system, $\rho(t)$, is obtained by taking the practical trace over dot-1, the apparatus. Thus we have $\rho(t) = \rho_{00}(t) + \rho_{11}(t)$. Our objective is to obtain a master equation for $\rho(t)$ alone.

Substitution of the ansatz equation (7) into the master equation gives a set of equations for the operators $\rho_{nm}(t)$. Taking care to maintain operator ordering we find

$$\frac{d\rho_{00}}{dt} = -i\Omega(c_2^\dagger \rho_{10} - \rho_{01} c_2) - 2\gamma_{L1}\rho_{00} + 2\gamma_{R1}\rho_{11}, \tag{8}$$

$$\frac{d\rho_{11}}{dt} = -i\Omega(c_2 \rho_{01} - \rho_{10} c_2^\dagger) + 2\gamma_{L1}\rho_{00} - 2\gamma_{R1}\rho_{11}, \tag{9}$$

$$\frac{d\rho_{10}}{dt} = -i\Omega(c_2 \rho_{00} - \rho_{11} c_2) - (\gamma_{L1} + \gamma_{R1})\rho_{10}, \tag{10}$$

$$\frac{d\rho_{01}}{dt} = -i\Omega(c_2^\dagger \rho_{11} - \rho_{00} c_2^\dagger) - (\gamma_{L1} + \gamma_{R1})\rho_{01}. \tag{11}$$

Note that the quantity of interest $\rho_{00} + \rho_{11}$ does not decay at all, but that the off-diagonal operators do decay. We then assume then that the off-diagonal operators rapidly achieve a steady state which are adiabatically followed by the diagonal operators. After a little algebra one finds for the reduced system density operator ρ that

$$\frac{d\rho}{dt} = \frac{\Omega^2}{\gamma}\left(2c_2^\dagger \rho_{11} c_2 + 2c_2 \rho_{00} c_2^\dagger - \rho_{00} c_2^\dagger c_2 - c_2^\dagger c_2 \rho_{00} - c_2 c_2^\dagger \rho_{11} - \rho_{11} c_2 c_2^\dagger\right). \tag{12}$$

If we now assume that $\gamma_{R1} >> \gamma_{L1}$, a self-consistent check reveals that $tr(\rho_{11}) \approx 0$, indicating that in this limit there is very little probability of finding an electron on dot-1. This means we can set $\rho_{11} > 0$ and $\rho \approx \rho_{00}$. We thus finally obtain the master equation for the measured system alone,

$$\frac{d\rho}{dt} = \frac{\Omega^2}{\gamma}\mathcal{D}[c_2]\rho, \tag{13}$$

where $\gamma = \gamma_{L1} + \gamma_{R1}$.

In this form we see that the effect of the measurement is to cause a decay of excitation in the measured system. This is in contrast to the measurement model using a single electron transistor discussed by Wiseman *et al.* (2000) where the effect of the measurement does not change the occupancy of the measured dot, but does induce the phase decay of any coherence between the measured dot and other parts of the system.

In the case considered here the measurement also destroys coherence between the measured dot and any other system with which it may have become correlated. To see this, suppose for example that dot-2 was initially entangled with another quantum dot, dot-3,

$$|\psi\rangle_{23} = \alpha|1\rangle_2 \otimes |0\rangle_3 + \beta|0\rangle_2 \otimes |1\rangle_3. \tag{14}$$

The degree of correlation between dots 2 and 3 is measured by $\langle c_2 {c_3}^\dagger \rangle$ which initially is equal to $\alpha\beta^*$. In the presence of the measurement, however, one finds that

$$\langle c_2 c_3^\dagger \rangle(t) = \alpha\beta^* e^{-\Omega^2 t/\gamma} \tag{15}$$

and any initial entanglement decays exponentially.

It is interesting to ask what happens to the measured current through the apparatus dot in the adiabatic approximation. After all, this should carry the signal if this system can be constructed as a measurement at all. The adiabatic approximation assumes that the tunnelling rates into and out of the apparatus dot are very large, so most of the time the current will be dominated by events originating in the leads of dot-1 and contain no reference to the measured system at all. The average instantaneous current through the apparatus dot (dot-1) is

$$i(t) = \frac{e}{2}(E(dN_{S1}(t)) + E(dN_{D1}(t))). \tag{16}$$

The connection between quantum and classical stochastic processes in the leads discussed above implies that

$$i(t)dt = e(\gamma_{R1}\langle c_1^\dagger c_1 \rangle + \gamma_{L1}\langle c_1 c_1^\dagger \rangle). \tag{17}$$

Using the ansatz equation (7), and recalling that we have also assumed that $\gamma_{R1} >> \gamma_{L1}$, it is easy to show that

$$\frac{di(t)}{dt} = e(\Omega^2\langle c_2^\dagger c_2 \rangle - \gamma_{R1}^2). \tag{18}$$

The first term is the signal. It is thus apparent that this scheme is a *absorptive* measurement of the number of electrons in the measured dot. The absorptive nature is embodied in the effective master equation equation (13) for the measured system alone. This should be contrasted with the case considered by Wiseman *et al.* (2000) based on a single electron transistor which measured the electron number in the measured dot, without absorption. The phase dependence in the case considered here ultimately results from the phase dependent coupling between the two dots and could be varied if a means could be found to change the phase of the coupling constant in the Hamiltonian describing the coherent tunnelling between the two dots.

3. Beyond the Adiabatic Approximation

The previous approximation scheme indicated in what sense we can regard one dot as a measuring apparatus for the other. In our simplified analysis, with only a single bound state on the measured dot, the measured signal is rather small. If there were very many electrons on the measured dot, the relation between the measured current and the occupation on the dot would still hold (so long as the electrons in dot-2 did not enter some strongly correlated many body state). Eventually, however every electron on the dot would tunnel onto the apparatus dot where it would be immediately dumped in the output current forming the signal. This is analogous to the destructive counting of photons in an optical cavity. Eventually the cavity, like the dot, is left in the vacuum, or zero-particle state.

To go further we need to introduce a continuous source of electrons for the measured system, dot-2. We now assume that this dot is connected to leads and biased reservoirs. However, these reservoirs are independent of those driving the measurement apparatus. In that case the fact that this system is functioning as a measurement should induce correlations between the currents in dot-1 and dot-2. The density operator for the total system, apparatus + dot, obeys the equation of motion (3) and therefore results in a system of sixteen coupled differential equations. On a physical basis many of these matrix elements can be eliminated. For simplicity, we assume the system begins in a pure state and the number of differential equations can therefore be reduced to five.

The steady state current was calculated analytically and is given by

$$i_{\infty}^{(n)} = \frac{1}{D}\Big\{\gamma_{Ln}\gamma_{Rn}\left[(\gamma_{Ln}+\gamma_{Rn})(\gamma_{Lm}+\gamma_{Rm}) + (\gamma_{Lm}+\gamma_{Rm})^2\right]$$

$$+2\Omega^2\left[\gamma_{Ln}\gamma_{Rm} + 2\gamma_{Ln}\gamma_{Rn} + \gamma_{Lm}\gamma_{Rn}\right]\Big\}\,, \tag{19}$$

where $D = [(\gamma_{L1}+\gamma_{R1})(\gamma_{L2}+\gamma_{R2}) + 4\Omega^2] \times (\gamma_{L1}+\gamma_{L2}+\gamma_{R1}+\gamma_{R2})$ and

$$m = \begin{cases} n+1, \text{ if } n=1 \\ n-1, \text{ if } n=2\,. \end{cases}$$

The two-time correlation function of the current through the apparatus dot (dot-1) $i^{(1)}(t)$ is

$$G(\tau) = \left\langle i^{(1)}(t), i^{(1)}(t+\tau)\right\rangle_{t\to\infty}\,. \tag{20}$$

Substitution of equation (4) into (12) gives the first term as

$$\langle i(t)i(t+\tau)\rangle_{t\to\infty}\, dt^2 = \frac{e^2}{4}\,\langle dN_E(t)dN_E(t+\tau) + dN_E(t)dN_C(t+\tau)$$

$$+dN_C(t)dN_E(t+\tau) + dN_C(t)dN_C(t+\tau)\rangle_{t\to\infty}\,, \tag{21}$$

where the superscript (1) has been dropped. This can be reduced to

$$\left\langle i^{(1)}(t)i^{(1)}(t+\tau)\right\rangle_{t\to\infty} = \frac{e}{2}i_\infty\delta(\tau) + \left\langle i^{(1)}(t)i^{(1)}(t+\tau)\right\rangle_{t\to\infty}^{\tau\neq 0}. \tag{22}$$

Applying the theory of open quantum systems (Wiseman and Milburn 1993) gives

$$E\left(dN_E^{(1)}(t+\tau)dN_E^{(1)}(t)\right) = \gamma_L^{(1)}\gamma_L^{(1)}\mathrm{Tr}\left\{c_1c_1^\dagger e^{\mathcal{L}\tau}\, c_1^\dagger\rho_\infty c_1\right\}dt^2, \tag{23}$$

$$E\left(dN_E^{(1)}(t+\tau)dN_C^{(1)}(t)\right) = \gamma_L^{(1)}\gamma_R^{(1)}\mathrm{Tr}\left\{c_1c_1^\dagger e^{\mathcal{L}\tau}\, c_1\rho_\infty c_1^\dagger\right\}dt^2, \tag{24}$$

$$E\left(dN_C^{(1)}(t+\tau)dN_E^{(1)}(t)\right) = \gamma_R^{(1)}\gamma_L^{(1)}\mathrm{Tr}\left\{c_1^\dagger c_1 e^{\mathcal{L}\tau}\, c_1^\dagger\rho_\infty c_1\right\}dt^2, \tag{25}$$

$$E\left(dN_C^{(1)}(t+\tau)dN_C^{(1)}(t)\right) = \gamma_R^{(1)}\gamma_R^{(1)}\mathrm{Tr}\left\{c_1^\dagger c_1 e^{\mathcal{L}\tau}\, c_1\rho_\infty c_1^\dagger\right\}dt^2, \tag{26}$$

where $e^{\mathcal{L}\tau}c_n\rho_\infty c_n^\dagger = \rho(\tau)$ with the initial condition $\rho(0) = c_n\rho_\infty c_n^\dagger$. The time-dependent density operator was determined by solving the system of five differential equations representing the master equation with the corresponding initial condition. The noise power spectrum $S(\omega)$ for each dot was then determined by the Fourier transform of the corresponding two-time correlation function. The deviation from shot-noise is a measure of electron–electron correlations between the source and drain events. We can determine the extent to which such correlations are important by calculating the Fano factor, which is the power spectrum normalised to shot noise

$$F(\omega) = \frac{S(\omega)}{2ei_\infty}. \tag{27}$$

The Fano factor $F(\omega)$ was numerically calculated and plotted against the frequency ω normalised by the rate $\gamma_L^{(1)}$. A third parameter was varied to produce a three-dimensional plot.

Typical noise spectra for the upper-dot in the coupled dot system are depicted in Figs 2 and 3 and are briefly analysed as follows. The spectrum exhibits distinct dips or valleys. The valleys are a direct result of the correlations, more precisely anticorrelations, between electron occupation of the bound state at different times. These anticorrelations reduce the randomness of electron transport through the device and therefore decrease the noise to a greater extent than already observed for the single quantum well (Sun and Milburn 1998). For large ω the spectrum approaches 0.5. This is due to the assumed form of the current obtained by the Ramo–Shockley theorem. For $\Omega \to 0$, the analytical expressions of the

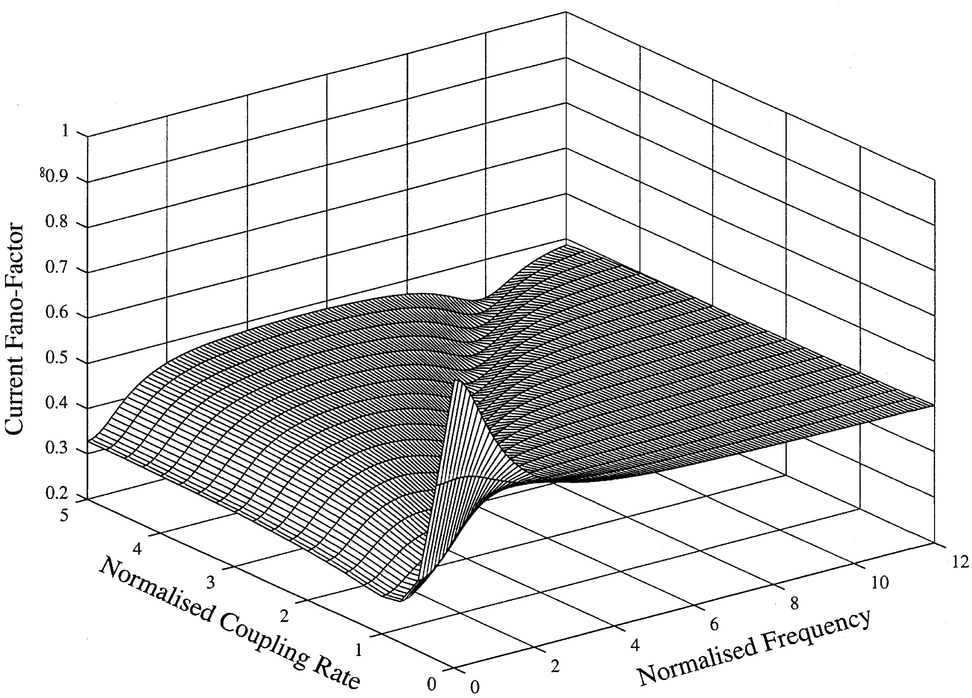

Fig. 2. Effect of the coupling rate on the current noise spectrum of coupled dots: the current Fano factor $F(\omega)$ versus the normalised frequency $\omega/\gamma_L^{(1)}$ and the normalised coupling rate $\Omega/\gamma_L^{(1)}$, when the other parameters are fixed: $\gamma_L^{(1)} = 1.0$, $\gamma_L^{(2)} = 0.1$, $\gamma_R^{(1)} = 0.1$ and $\gamma_R^{(2)} = 1.0$.

Fano factor for $i^{(1)}(t)$ and $i^{(2)}(t)$ reduce to that of a single quantum dot as expected in this limit.

The effects of the coupling Ω were examined by keeping all other parameters constant, as shown in Fig. 2.

For the case $\Omega >> \gamma$, there is increased noise suppression corresponding to $\omega = 2\Omega$. The reason for this is that when the coherent coupling dominates, it causes electrons, after entering a dot, to coherently tunnel into the other dot at the rate Ω. There will be a high probability that the electron will return to the original dot at the same rate as it left, since the coupling is much larger than any of the emission rates. Thus the electron will periodically cycle through each dot at a frequency 2Ω, suppressing any other electrons trying to enter either dot at this frequency. Thus for large coupling, the noise suppression at $\omega = 2\Omega$ is expected. The spectrum changes as the coupling is decreased and becomes comparable to that of the rates γ_{Ln} and γ_{Rn}. The coupling no longer dominates so that the probability of the electron periodically coherently tunnelling is approximately the same as the probability of the electron leaving a dot into one of the drains. This causes the spectrum to include more complicated features, such as the minimum of the dips being shifted from $\omega = 2\Omega$. This is illustrated explicitly at $\Omega = 2$, where the dip does not occur exactly at twice the coupling. Of course as $\Omega \to 0$, the characteristics of the spectrum approach that of a single dot, i.e. an increase of noise approaching that of full shot noise at low frequencies.

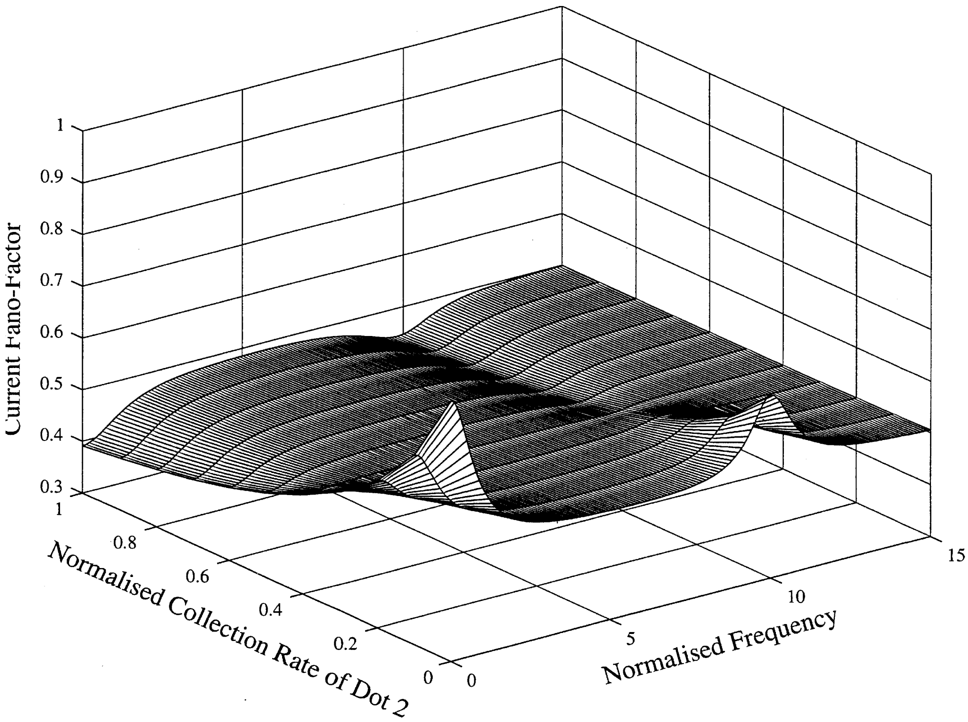

Fig. 3. Effect of the collection rate of $\gamma_R^{(2)}$ on the current noise spectrum of the upper dot: the current Fano factor $F(\omega)$ versus the normalised frequency $\omega/\gamma_L^{(1)}$ and the collection rate $\gamma_R^{(2)}/\gamma_L^{(1)}$, when the other parameters are fixed: $\gamma_L^{(1)} = 1.0$, $\gamma_L^{(2)} = 0.1$, $\gamma_R^{(1)} = 0.1$ and $\Omega = 5.0$.

To understand the characteristics of the spectrum, with variation of the rates, a particular case was chosen as an example. Fig. 3 shows the frequency dependence of the current Fano factor on the emission rate of the drain of dot-2, the measured system, γ_{R2}, with the other rates and coupling fixed ($\Omega = 5\gamma_{L1}$).

For all values of the rate γ_{R2} and frequency, the noise is suppressed due to correlations caused by the Pauli exclusion principle. As $\gamma_{R1} = 0.1$ is much smaller than $\gamma_{L1} = 1$, the current $i^{(1)}$ is governed by γ_{R1} and is therefore dominated by a Poisson process at low frequencies. For γ_{R2} small, the system is reduced to the case in Sun and Milburn (1998). The system is dominated by γ_{R2} and random for the same reason. This is the origin of the peaks at $\gamma_{R2} = 0$. An interesting feature to note is that the transition involves a point at which the spectrum characteristics are flat with an amplitude $F(\omega) = 0.5$. This particular feature is observed when the lower dot is symmetric, i.e. when $\gamma_L{}^{(2)} = \gamma_{R2}$, which is similar behaviour to that exhibited by a symmetric single dot.

Since the dots are coupled it can be expected that the current through the dots should be correlated. That is, not only can the time of arrival of electrons in each of the upper and lower collectors be separately correlated, but the time of arrival of electrons *between* each drain can be correlated. This is why the system can be treated as a measurement at all. In a similar manner as the two-time correlation function, the cross-correlation function representing the correlation between $i^{(1)}(t)$ and $i^{(2)}(t)$ can be introduced:

$$\begin{aligned} C_1(\tau) &= \left\langle i^{(1)}(t), i^{(2)}(t+\tau) \right\rangle_{t\to\infty} \\ &= \left\langle i^{(1)}(t) i^{(2)}(t+\tau) \right\rangle_{t\to\infty} - i_\infty^{(1)} i_\infty^{(2)}. \end{aligned} \tag{28}$$

This function is a measure of the relationship between $i^{(1)}$ at time t and $i^{(2)}$ at a later time $t + \tau$. Similarly, the correlation between $i^{(2)}(t)$ and $i^{(1)}(t + \tau)$ can be considered:

$$C_2(\tau) = \left\langle i^{(2)}(t), i^{(1)}(t+\tau) \right\rangle_{t\to\infty}. \tag{29}$$

Both the cross-correlation functions have a corresponding spectrum called the cross-correlation spectrum given by

$$R_n(\omega) = 2\int_0^\infty C_n(\tau)(e^{i\omega\tau} + e^{-i\omega\tau})d\tau \tag{30}$$

As the cross-correlation spectrum is a measure of the fluctuations between the two currents it can have both positive and negative values. The Fano factor for the cross-correlation spectrum is given by

$$F_n(\omega) = \frac{R_n(\omega)}{2e\sqrt{i_\infty^{(1)} i_\infty^{(2)}}}.$$

To find the cross-correlation spectra $R_n(\omega)$ and Fano factor $F_n(\omega)$, a similar method to find the noise spectrum was used. The cross-correlation spectra also exhibit peaks and valleys in their characteristics, but they do not represent an increase or decrease in the noise. A peak (a value greater than zero) represents a correlation between the fluctuations of the two currents where as a valley (a value less than zero) represents an anti-correlation.

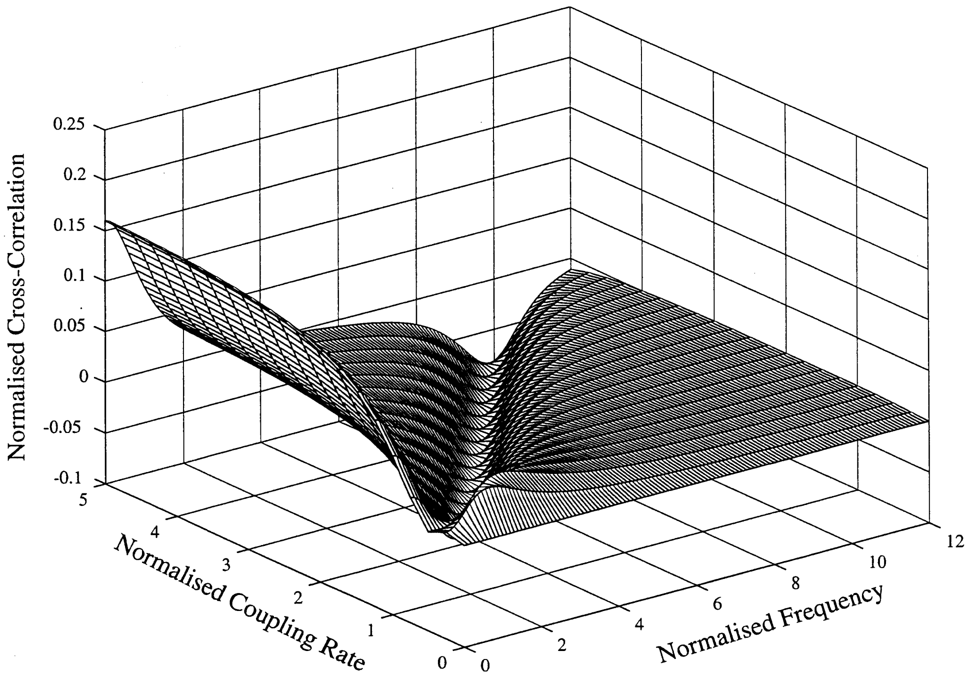

Fig. 4. Normalised cross-correlation spectrum $R_1(\omega)$ corresponding to $\langle i^{(1)}(t)i^{(2)}(t+\tau)\rangle$ versus the normalised frequency $\omega/\gamma_L^{(1)}$ and the normalised coupling rate $\Omega/\gamma_L^{(1)}$, when the other parameters are fixed: $\gamma_L^{(1)} = 1.0$, $\gamma_L^{(2)} = 0.1$, $\gamma_R^{(1)} = 0.1$ and $\gamma_R^{(2)} = 1.0$.

Figs 4 and 5 show the dependence of the cross-correlation spectra on the coupling Ω and the emission rate γ^{L2} respectively.

From Fig. 4 one can see that when the coupling is set to zero, the cross-correlation spectrum is flat at $R_n(\omega) = 0$. This is as expected since there should be no correlations between the currents. An increase in Ω has the same effect on both the cross-correlation spectra as it did on the noise spectrum (Fig. 4). The cross-correlation spectrum $R_2(\omega)$ corresponding to $\langle i^{(2)}(t)i^{(1)}(t+\tau)\rangle$ has very similar characteristics.

At about $\Omega = 5$ the two currents are highly anti-correlated for $\omega = 2\Omega$ and again this is due to electrons being periodically transferred between the two dots at the tunnelling frequency. A suppression of any other electrons entering either dot at a frequency $\omega = 2\Omega$ will occur and therefore an anti-correlation between the currents at a frequency twice the coupling is observed. As Ω approaches zero the spectrum begins to flatten since the currents become less dependent on each other.

The effect of the emission rates on $R_1(\omega)$, i.e. the spectrum corresponding to $C_1(\tau) = \langle i^{(1)}(t)i^{(2)}(t+\tau)\rangle$, was examined, and a special case is chosen for discussion. Fig. 5 shows the effect of the emission rate γ_{L2} on the spectrum $R_1(\omega)$ with coupling Ω and other rates fixed. This has very similar characteristics to that just discussed.

The anticorrelations at $\omega = 2\Omega$ remain in Fig. 5 for the reasons previously given. In this case γ_{L1}, γ_{R1}, and γ_{R2} are all equal to 1. When γ_{L1} is small it dominates and current fluctuation is significant. Therefore the cross-correlation is high at low frequencies. The

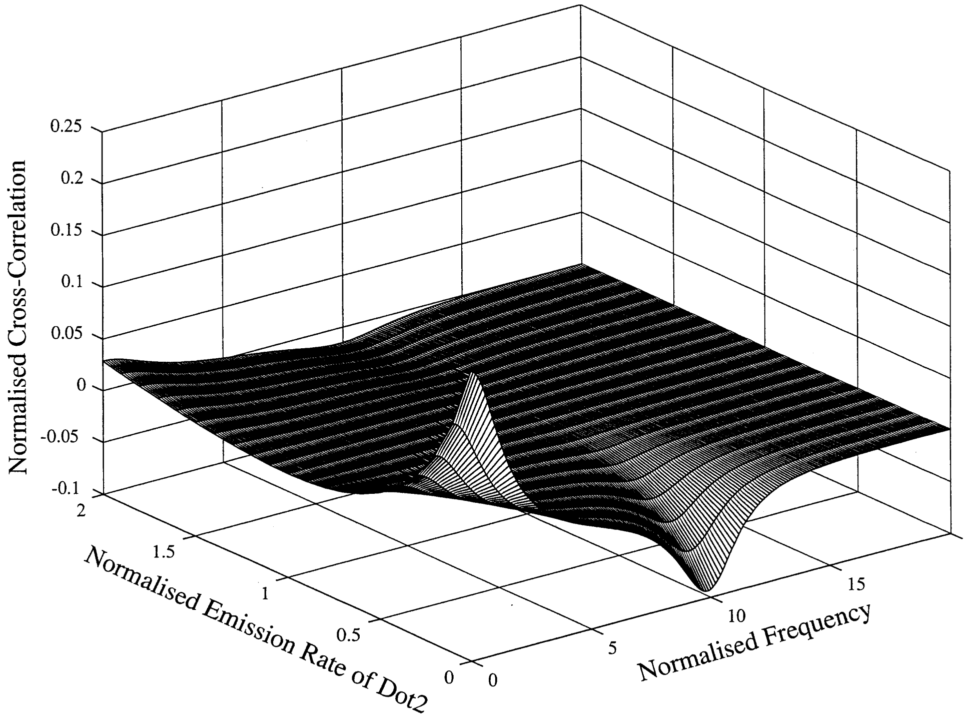

Fig. 5. Normalised cross-correlation spectrum $R_1(\omega)$ corresponding to $\langle i^{(1)}(t)i^{(2)}(t+\tau)\rangle$ versus the normalised frequency $\omega/\gamma_L^{(1)}$ and the emission rate $\gamma_L^{(2)}/\gamma_L^{(1)}$, when the other parameters are fixed: $\gamma_L^{(1)} = 1.0$, $\gamma_R^{(1)} = 1.0$, $\gamma_R^{(2)} = 1.0$ and $\Omega = 5.0$.

increase of γ_{L2} causes the probability of occupation of the both dots to approach one. Therefore an electron leaving the upper dot creates a vacancy for electrons to enter from the lower dot. This in turn leaves a vacancy in the lower dot which is quickly filled by low frequency electrons if γ_{L2} is large. Thus small correlations can occur for low frequencies.

A more interesting type of correlation function called the symmetrised cross-correlation function can also be used to analyse the system. It is defined as

$$C_s(\tau) = \frac{1}{2}\left[\left\langle i^{(1)}(t), i^{(2)}(t+\tau)\right\rangle_{t\to\infty} + \left\langle i^{(2)}(t), i^{(1)}(t+\tau)\right\rangle_{t\to\infty}\right], \tag{31}$$

with the corresponding spectrum defined as

$$R_s(\omega) = 2\int_0^\infty C_s(\tau)(e^{i\omega\tau} + e^{-i\omega\tau})d\tau \tag{32}$$

$$= \frac{1}{2}\left[R_1(\omega) + R_2(\omega)\right]. \tag{33}$$

This type of correlation function and spectrum allows the relationship between the two currents to be considered as being dependent on each current at *any* time. It effectively transforms the cross-correlation functions so that they are symmetrical. The spectra observed are very similar to the cross-correlation spectra and the same arguments used to explain the characteristics apply here as well. The importance of the summarised spectrum is that it is very sensitive to the entanglement between two coherently coupled qubits (Loss and Sukhorukov 1999).

The symmetrised cross-correlation function can be used to test and/or verify the nature of the two correlated quantities: quantum or classical? In the present case the two quantities are the currents of two dots, and the results show they are indeed classical in nature, i.e.

$$\frac{|C_s(\tau)|}{\frac{1}{2}[C_1(\tau)+C_2(\tau)]} < 1.$$

4. Conclusion

Coupled quantum dots are becoming important because of possible applications in quantum information processing and other areas. In this paper we have proposed a new application: an absorptive electron number measurement scheme. A model to describe coherent and incoherent transport in a quantum dot (Sun and Milburn 1999) is extended to a system of two single dots coherently coupled in parallel. One of the dots functions as a measurement apparatus and the other is the target to be measured. Applying the quantum theory of open systems identifies a relation between the experimentally measurable quantity, the current through the apparatus dot, and the quantum stochastic processes inside the dots. The analysis shows the measurement is absorptive in nature unlike the measurements based on single electron transistors (Wiseman *et al.* 2000). We have demonstrated that the proposed measurement process can be fully described by master equations applied to the whole system. This model has enabled the dynamics of coupled quantum dot systems to be specified within the Markov and weak coupling limits. Numerical results provide visualised pictures of the influence of relevant parameters on the spectra. These can be used to predict the experimental results if the parameters are known, or to obtain the relevant unknown parameters from the measurement results. For example, from the valley of the noise spectrum one can extract the coupling rate between two quantum dots.

References

Aleiner, I. L., Wingreen, N. S., and Meir, Y. (1997). *Phys. Rev. Lett*. **79**, 3740.

Bandyopadhyay, S., Das, B., Miller, A. E. (1994). *Nanotechnology* **5**, 113.

Blick, R. H., *et al*. (1996). *Phys. Rev.* B **53**, 7899.

Buks, E., Schister, R., Heiblum, M., Mahalu, D., and Umansky, V. (1998). *Nature* **391**, 871.

Datta, S. (1995). 'Electronic Transport in Mesoscopic Systems', pp. 247–8 (Cambridge Univ. Press).

Elattari, B. and Gurvitz, S. A. (2000). *Phys. Rev. Lett.* **84**, 2047.

Fujisawa, T., and Tarucha, S. (1997). *Superlattices Microstructures* **21**, 247.

Gardiner, C. W. (1983). 'Handbook of Stochastic Methods', pp. 34, 42 (Springer: Berlin).

Gurvitz, S. A. (1997). *Phys. Rev.* B **56**, 15215.

Lent, C. S. and Tougaw, P. D. (1993). *J. Appl. Phys.* **74**, 6227.

Loss, D., and Sukhorukov, E. V. (2000). *Phys. Rev. Lett*. **84**, 1035.

Luryi, S. (1991). *IEEE J. Quant. Electron.* **27**, 54.

Milburn, G. J. (2000). *Aust. J. Phys.* **53**, 477.

Milburn, G. J., and Sun, H. B. (1998). *Contemporary Phys.* **47**, 67.

Nomoto, K., Ugajin, R., Suzuki, T., and Hare, I. (1996). *J. Appl. Phys.* **79**, 291.

Openov, L. A., and Bychkov, A. M. (1998). *Phys. Low-dimensional Structures* **9–10**, 153.

Ramo, S. (1939). *Proc. IRE* **1939**, 584.

Shockley, W. (1938). *J. Appl. Phys.* **9**, 635.

Sprinzak, D., Buks, D., Heiblum, E., and Shtrikman, H. (2000). *Phys. Rev. Lett.* **84**, 5820.
Sun, H. B., and Milburn, G. J. (1998). *Superlattices Microstructures* **23**, 883.
Sun, H. B., and Milburn, G. J. (1999). *Phys. Rev.* B **59**, 10748.
Wiseman, H. M., and Milburn, G. J. (1993). *Phys. Rev.* A **47**, 1652.
Wiseman, H. M., Utami, D. W., Sun, H. B., Milburn, G. J., Kane, B., Clark, R., and Dzurak, A. (2000). *Phys. Rev.* B (in press).

Manuscript received 17 April, accepted 14 August 2000